Prebiotic synthesis of phosphoenol pyruvate by α-phosphorylation controlled triose glycolysis

Adam J. Coggins[1] and Matthew W. Powner[1]

[1] Department of Chemistry, University College London, 20 Gordon Street, London, WC1H 0AJ, UK

Phosphoenol pyruvate is the highest-energy phosphate found in living organisms and is one of the most versatile molecules in metabolism. Consequently, phosphoenol pyruvate is an essential intermediate in a wide variety of biochemical pathways, including carbon fixation, the shikimate pathway, substrate-level phosphorylation, gluconeogenesis and glycolysis. Triose glycolysis (generation of ATP from glyceraldehyde 3-phosphate via phosphoenol pyruvate) is amongst the most central and highly conserved pathways in metabolism. Here, we demonstrate the efficient and robust synthesis of phosphoenol pyruvate from prebiotic nucleotide precursors, glycolaldehyde and glyceraldehyde. Furthermore, phosphoenol pyruvate is derived within an α-phosphorylation controlled reaction network that gives access to glyceric acid 2-phosphate, glyceric acid 3-phosphates, phosphoserine and pyruvate. Our results demonstrate that the key components of a core metabolic pathway central to energy transduction and amino acid, sugar, nucleotide and lipid biosyntheses can be reconstituted in high yield under mild, prebiotically plausible conditions.

The integrated pathways of metabolism are orchestrated by an array of enzymes and chaperones that are ultimately dependent on a highly evolved genetic coding system essential to all life on Earth. However, at the origins of life, before the advent of sophicated enzymatic catalysis and selection, metabolism was required to provide the fundamental building blocks of life.[1-14] Although only an intriguingly small constellation of molecules produce the diversity of contemporary life, the function of the individual biological components cannot be appreciated in isolation.[1,2] Therefore, it must follow that the generation and function of biochemical species at the origins of life requires a concerted and, ideally, unified investigation.[14] Seeking to further establish the prebiotic generational relationship between the essential molecular components of biology, we were struck by the constitutional relationship between nucleotide precursors glycolaldehyde (**2**) and glyceraldehyde (**3**) and the carbon framework of phosphoenol pyruvate (**1**), biology's highest-energy phosphate (free energy at pH 7, 25 ºC ($kJmol^{-1}$): **1**=-61.9; creatine phosphate=-43.0; adenosine triphosphate=-30.5; pyrophosphate=-19.2; glucose-6-phosphate=-13.8).[15-18]

Pyruvate (**6**) synthesis has been reported at elevated temperatures (250 °C) and pressures (50–200 MPa) in the presence of iron sulfides (0.07% yield),[19] during the abiotic degradation of sugars and sugar-phosphates,[20,21] and in good yield by lactic acid oxidation (70%).[22] However, access to the high-energy phosphate **1** required by metabolism has not been addressed. Although phosphorylation of glyceric acid (**4**) by cyclotrimetaphosphate—that, notwithstanding contrary opinion,[30] is considered a promising prebiotic phosphorylating agent[23-29]—yields a 1:1.2 mixture of glyceric acid 2- and 3-phosphates (**4-2P**/**4-3P**; 38%)[23] and amide derivatives can be accessed by Passerini reactions,[31] the elimination of **4-2P** (or its amide derivatives) to give **1** has not been demonstrated. Indeed, even under strongly acidic (pH 2), alkaline (pH 10) or general acid-base

(1M phosphate, pH 7) conditions, **4-2P** (60mM) is remarkably stable for prolonged periods of incubation (>15 hours at 60 ºC; Supplementary Fig. 1). To overcome the shortcomings of both regioselective phosphorylation and elimination, we reasoned that **1** would be directly accessible with high efficiency and complete regiochemical control by mild, aldehyde-mediated reactivity and late-stage oxidation. Amidotriphosphate (**7**) and diamidophosphate (**8**)—the ammonolysis products of cyclotrimetaphosphate[23-32]—effect a remarkably selective phosphorylation of α-hydroxyaldehydes and sugars in aqueous solution,[25,32] and are commonly regarded to be prebiotically plausible.[24,25,28-32] It was of particular interest to us that these phosphorylations block entry of the key aldehyde components **2** and **3** into ribonucleotide syntheses,[1,18] which redirects both **2** and **3** to non-natural phosphorylation patterns and pyranosyl (rather than natural furanosyl) sugar and nucleotide structures.[33] In a seminal contribution to prebiotic chemistry, Eschenmoser and co-workers outlined the possibility that this switch in reactivity could have predisposed the prebiotic synthesis to non-canonical nucleotides.[25,32-34] However, by contrast we hypothesised that α-phosphorylation would redirect **2** and **3** into another metabolic pathway, and provide a generational link between two distinct pathways within (proto)metabolism. Specifically, under prebiotically plausible conditions,[18] rapid dehydration of glyceraldehyde 2-phosphate (**3-2P**) was anticipated to yield phosphoenol pyruvaldehyde (**9**) and, upon oxidation, **1**. Interestingly, given the central role of glycolysis in shaping biochemical amino acid, nucleotide and lipid syntheses and the metabolic relationship between **3**, **4-2P**, **4-3P**, **1** and **6**, the efficient generation of each species is observed after subtle variations of mild aqueous reaction conditions to establish a single chemical network that can assemble each of the components of the triose glycolysis pathway of contemporary metabolism (Fig. 1).

Results

Phosphoenol pyruvaldehyde (9): Eschenmoser and co-workers reported the phosphorylation of tetrose and pentose sugars with **8**,[32] and magnesium-dependent phosphorylation of **2** and **3** with **7**.[25] We have found that the pH-stabilisation provided by phosphate buffer (pH 7), as anticipated, removes the reported[32] requirement for periodic addition of both **8** and a proton-exchange resin during diamidophosphate-mediated phosphorylations (to counteract the stoichiometric liberation of ammonia and ensure that the phosphorylation reaction proceeds). Phosphate-buffered phosphorylation of **2** (25mM) by **8** (100mM) at ambient temperature gave clean phosphorylation after 22 hours. However as both imine formation and amidophosphate protonation appear essential to the mechanism of phosphorylation, we suspected that the reaction could be promoted at lower pH. Accordingly, we observed an optimal rate of conversion at pH 4 that gave 90–96% phosphorylation of **2** or **3** (25mM) at ambient temperature in two hours (Supplementary Fig. 4). Upon incubating **3-2P** (80mM) in phosphate (0.5M) we observed facile dehydration to **9** (74%, 1 d, 60 ºC; Supplementary Fig. 21). Furthermore, direct synthesis of **9** (50%) was observed during the stoichiometric phosphorylation of **3** in phosphate buffer (pH 4, 0.5M, 60 ºC, 5 d) to directly establish the high-energy phosphoenol moiety of **1** under mild aqueous conditions.

Having demonstrated the synthesis of **9** from **3**, we next incubated glycolaldehyde phosphate (**2-P**) with formaldehyde. At pH 10.7 **2-P** is converted to **3-2P** (66%) over the course of 6 days;[33] we observed that further incubation (60 ºC, pH 10, 3 d) leads to elimination to furnish **9** (61%; Supplementary Fig. 22). Alternatively, incubation in phosphate buffer (0.5M, 60 ºC, pH 7, 30 h) led to the direct synthesis of **9** (40%; Supplementary Fig. 23) from formaldehyde and **2-P**. Demonstrating the phosphorylation of both prebiotic aldehyde precursors of RNA can lead, even at neutral pH, to high-energy phosphenol ether **9**.

Phosphoenol pyruvate (1): Struck by the simplicity and efficiency of this synthesis and the structural relationship between **9** and **1**, we next turned our attention to the oxidation of **9**. The range of potential conditions and oxidants available under prebiotic constraint is unknown and likely highly varied. Therefore, rather than develop a model geochemical scenario for aldehyde oxidation, we sought to demonstrate a range of low temperature, aqueous model oxidations that operate through significantly varied mechanistic pathways across a broad pH range (pH 3 – 13). Activation towards oxidation through cyanohydrin formation[35] initially appealed to us because high concentrations of hydrogen cyanide are implicated in nucleotide, sugar and amino acid abiogenesis[1,5,8,12] and are observed in abiotic high abundance.[36,37] Incubation of **9** (33–200mM) with sodium cyanide (167mM –1M) led to rapid (<15 min) and quantitative conversion to cyanohydrin **10** in water (Supplementary Fig. 33). Because iron is likely to be prebiotically abundant[21] and clearly has biological importance,[37] we first investigated ferricyanide ($[Fe(CN)_6]^{3-}$) oxidation of **10**. Ferricyanide is a prebiotically plausible model oxidant[12,39-42] that contains low-spin iron, which is easily reduced to the ferrocyanide ion ($[Fe(CN)_6]^{4-}$) in a reversible redox couple, and can be photochemically regenerated from ferrocyanide.[12,39,41] We were pleased to observe oxidation of **10** by ferricyanide between pH 11 and 13 (Fig. 2 & Supplementary Fig. 36). However, expedient oxidation required significantly elevated pH and became limited by alkaline nitrile hydrolysis.

To further improve the oxidation reaction and expand the scope of potential model oxidants, we next investigated manganese, which is the most common heavy metal in the Earth's crust (0.1 wt %) after iron,[43] and readily adopts +2, +3, +4, +6 and +7 oxidation states, although naturally occurring systems are dominated by +2, +3, and +4 oxidation states. Manganese is abundant in most geological systems, covers 10–30% of the deep Pacific Ocean floor,[44] and is readily found

in minerals such as birnessite, pyrolusite, romanechite and todorokite.[43,44] Additionally, phylogenetic analysis suggests that manganese may have been the active center of the earliest enzymes,[38] and manganese concentrations are thought to have been as high as 50mM in the oceans of the early Earth.[44] Although the global availability of redox sensitive Mn(IV) prior to atmosphere oxygenation has been questioned,[45-47] the deviation of local environments and near-surface oxygen fugacity from global values[48] (e.g. owing to photo-oxidation, ionization, volcanic outgassing, meteorite impacts and atmospheric water dissociation and hydrogen escape) remains opaque.[49] However, stimulated by the recent elucidation of facile prebiotically plausible sugar, amino acid and lipid syntheses mediated by photo-oxidation of transition metals in aqueous solution,[12,39,41] and recognizing the prebiotically plausible (photo-)oxidation of Mn(II) to Mn(III) and Mn(IV),[50,22] and disproportionation of Mn(III) to Mn(II) and MnO_2 in the absence of complexing ligands, manganese dioxide (MnO_2) was investigated as the most constitutionally simple Mn(IV) oxidant. Interestingly, we observed near-quantitative conversion of **9** (100mM) to **1** (93%) upon incubation with potassium cyanide (500mM) and manganese dioxide (20 eq.) after two hours, which demonstrates the facile synthesis of **1** from both **2** and **3** (Fig. 2 & Supplementary Fig. 37).

We next investigated the direct chemical oxidation of **9** to **1**. The relatively low bond-dissociation energy of an aldehyde hydrogen atom (360-370 $kJmol^{-1}$),[51] likely high prebiotic availability of iron[21] and prebiotic plausibility of a hydroxyl-radical-mediated oxidation,[24,52] suggested the investigation of Fenton oxidation. Interestingly, incubation of **9** (25mM) with ferrous chloride (25mM) and hydrogen peroxide (100mM) at pH 7 – 11 furnished **1** (30%, 25 ºC, pH 10; Fig. 2 & Table 1). However, these aggressive oxidation conditions also led to the concomitant degradation of **1** to formate and glycolate (**12**).

To make further improvements to the direct oxidation, guided by the conditions of nucleotide synthesis,[14,18] the prevalence of dry heating and wet-dry cycles in prebiotic synthesis,[12,14,18,29,53] and the simple photochemical synthesis and high abiotic abundance of the chlorate family of molecules,[54-57] we were drawn to investigate the role of these abiotic oxidants. Chlorates are ubiquitously formed by stratospheric oxidation of chlorides on Earth, and are widely distributed by both wet and dry deposition.[57] Although ozone likely plays a key role on Earth today, chlorates are also widely distributed throughout the solar system (on Mars, the Moon and carbonaceous chondrites, including Murchison and Fayetteville). Little is yet known regarding the origin of chlorates on Mars, however the known terrestrial syntheses do not account for their abundance or distribution throughout the solar system.[54,55,57] Therefore, although the arid environments implicated in chlorate synthesis are debated and the delivery of chlorates to prebiotic chemistry remains unknown, there are clearly abiotic mechanisms for the accumulation of chlorates, which, if followed by wetting, could potentially either mobilize deposits or deliver materials to chlorate-rich locations. Moreover, the disproportionation of atmospheric ClO_2 in aqueous solutions would directly deliver chlorite,[56,58] which is an excellent mild oxidant for aldehydes in water with a pH reactivity profile that is an ideal match for **8**-mediated phosphorylation.[59] Therefore, despite the uncertain provenance of chlorates in prebiotic chemistry, the abundance of chlorates in the solar system and their capability to act as mild and highly selective nucleophilic oxidants in water meant that we judged chlorates to be an interesting model oxidant for **9**. Chlorite oxidation of aldehydes can be mediated at low pH (pH 3–6) in the presence of a phosphate buffer, which allows a transition away from high-pH cyanide-catalysed oxidations. Upon incubation of **9** (70mM) with chlorite (100mM) and a

hypochlorite scavenger such as methionine (140mM) or DMSO (140mM), **9** is quantitatively oxidized to **1** (Supplementary Figs. 39–40).

Glyceric acid 2-phosphate (4-2P) and glycolic acid phosphate (12-P): Gratifyingly, the oxidation by chlorite is general and provides quantitative conversion of **2** and **2-P** to glycolic acid (**12**) and glycolic acid phosphate (**12-P**), respectively (Table 1 & Supplementary Figs. 41–42); Phosphate **12-P** is a key intermediate of photorespiration in plants.[15] Consequently, chlorite is also an ideal oxidant to convert **3-2P** to **4-2P**. Upon reaction of **3-2P** with stoichiometric chlorite, we observed quantitative oxidation to **4-2P**. Furthermore, upon phosphorylation of **3** with **8** followed by incubation at 60 ºC in phosphate buffer (0.5M) for 5 hours, and addition of chlorite/DMSO (1:1.4), we observed quantitative conversion of **3** to **1** and **4-2P** (1:1) and realized the direct divergent synthesis of two key intermediates of the universally conserved glycolysis pathway (Fig. 3).[17]

Glyceric acid 3-phosphate (4-3P) and phosphoserine (5-3P): Interestingly, the hydrolysis that limited the ferricyanide oxidation of cyanohydrin **10** suggested direct prebiotic access to **4-3P** and phosphoserine (**5-3P**) through cyanohydrin and aminonitrile hydrolysis, which provides access to a fourth component of the glycolysis pathway and a direct link to serine metabolism, repsectively. Upon incubation of **2-P** with sodium cyanide, we observed smooth and quantitative conversion to cyanohydrin **14** (Supplementary Fig. 46), which is readily hydrolysed to **15** (27%, 750mM phopshate, pH 7, 3 d, 75 ºC; Supplementary Fig. 54), and to **4-3P** (31%, 750mM phopshate, pH 12, 75 ºC, 5 h; Supplementary Fig. 59) with absolute control over the phosphate regiochemistry (Fig. 4).

Furthermore, incubation of **2**-P with ammonium cyanide led to the near-quantitative synthesis of glycolaldehyde phosphate aminonitrile (**16**; Supplementary Fig. 66). We found that the

hydrolysis of aminonitrile **16** to amide **17** was aldehyde catalysed; the cyanide carbon atom was mildly and efficiently locked into the carbon framework of serine by a small excess of **2-P** (<5%).[60] This reactivity is only observed for aminonitrile hydrolysis, not cyanohydrin hydrolysis; the aldehyde-catalysed hydrolysis occurs via 5-*exo*-*dig* hemiaminal cyclisation and is quenched by excess cyanide. Therefore, it is of note that we observed no evidence of intramolecular phosphate-assisted hydrolysis, despite the ostensive potential for 6-*exo*-*dig* addition to the nitrile, which would stall **5-3P** synthesis at glycolic acid **4-3P**, and as a result we observed efficient conversion of **2-P** to **5-3P** (36%; Supplementary Fig. 83).

Pyruvate (6): Compound (**1**) is highly stable at high pH (6% hydrolysis to **6** observed over 2 d at pH 10 and 60 ºC; Supplementary Fig. 93). However, **1** is readily hydrolysed to **6** at lower pH in quantitative yield (pH 4–7, 2 d, 60 ºC; Supplementary Fig. 94). Hydrolysis provides access to a second linchpin of contemporary metabolism with excellent control and efficiency in water. Accessing **6** from **1** delivers improved yields (up to 69% from **3**, over 4 steps) relative to previously reported multiple-step syntheses (984-fold and 7-fold),[19,20] and a comparable yield to the single-step oxidation of lactic acid (70%).[22] More importantly, the pathway mimics a metabolic trajectory with absolute specificity under mild aqueous conditions from simple prebiotic aldehydes.

Acetate (20): It is of significant interest that during our investigation of phosphoenol pyruvaldehyde (**9**) oxidation with chlorite that in the absence of a hypochlorite scavenger we observed over oxidation to give chloroacetate (**18**; >98% yield with 2 equivalents of chlorite; Supplementary Fig. 95). It is likely that **18** was accessed by electrophilic chlorination and oxidative decarboxylation of α-ketoacid **19** (Fig. 2), which is supported by the observed quantitative oxidative decarboxylation of **6** to yield **20**.[61] Pyruvates **1** and **6** are both key nodes of

central metabolism, but one of the most important metabolic connections is achieved by oxidative decarboxylation of **6** to access acetyl coenzyme A (**Acetyl CoA**),[62] ketogenesis and the citric acid cycle (Fig. 1).[6-9] The direct liberation of **20** by oxidation of **6** suggests an essential prebiotic link between C_3 and C_2 metabolism within our system; an investigation of (prebiotic) pathways to acetyl transfer reagents[40,42] and C_2-metabolism are currently underway in our laboratory.

Discussion

Glycolysis is one of the most highly conserved metabolic pathways of life, and it is instrumental to biosynthesis of amino acids, sugars, nucleotides and lipids, phosphorylation and the entry to the Krebs (citric acid) cycle.[2,16,17] The interrelated syntheses of **1**, **4**, **4-2P**, **4-3P**, **5-3P**, **6**, **12**, **12-P** and **20** demonstrated herein implies that prebiotic availability, as well as metabolic versatility, may have positioned glycolysis at the heart of modern cellular metabolism. The generational simplicity of this network also suggests that α-phosphorylation and oxidation warrant further investigation with respect to the essential roles they may have played in coordinating the first steps of life on Earth. Specifically, the remarkable chemical control that α-phosphorylation achieves in reconstituting the pathway of glycolysis indicates that a transition from α-phosphorylation to terminal phosphorylation may greatly simplify the transition from abiotic reactions to contemporary metabolism. The essential and ubiquitous roles of **4-2P** and **1** in modern biochemistry may be vestiges of an earlier reactivity upon which modern glycolysis/gluconeogenesis are built from the 'bottom up'.[17] Although modern metabolism enters triose glycolysis through glyceraldehyde 3-phosphate (**3-3P**), **3-3P** is unstable with respect to its ketose isomer (**21-P**) and is predisposed to undergo elimination to methyl glyoxal with concomitant loss of phosphate activation. Biochemically, the isomerisation of triose sugar

phosphates is mediated to the limit of diffusion by triose-phosphate isomerase, but at equilibrium formation of **21-P** is still favoured 20:1.[63] It is of note, however, that we have demonstrated that glyceraldehyde 2-phosphate (**3-2P**) blocks these deleterious reaction pathways without the requirement for enzymatic control. Furthermore, by retaining aldehyde activation to E1cb-type elimination, **3-2P** readily undergoes a predisposed elimination to access the high-energy phosphoenol moiety, which is kinetically prohibited for **4-2P** and its amide derivatives.

Aldehyde oxidations are commonplace in chemistry, and a variety of oxidants can be used in the facile oxidation of **9** to **1**. The conditions on the early Earth are far from certain, and we have not sought to specify geochemical constraints for aldehyde oxidation; we have, however, demonstrated *umpolung* and conventional polarity oxidation, nucleophilic, electrophilic and radical oxidation, heterogeneous and homogenous oxidation and both outer- and inner-sphere oxidation of **9** to give **1**, and consequently suspect that the facile oxidation of **9** in water is extremely general, and thus prebiotically plausible. Nonetheless, further investigation of redox-sensitive elements (including Mn, Fe, Co, Ni, and Cu) on the early Earth is warranted prior to unification of prebiotic and geochemical redox strategies.[49]

It is of note that the chlorite oxidation is not only quantitative but that its reactivity profile is also pH matched with the maximal reactivity of the prebiotic phosphorylating agent **8** (optimal α-phosphorylation at low pH). At the concentrations investigated (25–500mM), background hydrolysis does not compete with Schiff base mediated phosphoryl transfer, however, the increased efficiency of Schiff base formation and increased proportion of protonated amidophosphate leads to a significantly improved rate of phosphorylation. This pH profile also matches the pH requirements (pH < 7) for controlled ribonucleotide assembly by a leading model for prebiotic synthesis.[18] Therefore, it is also interesting to note that an acidic drying phase is

required during ribonucleotide synthesis to induce phosphorylation and stereocontrolled rearrangement,[14,18] and these arid, low-pH conditions have remarkable parity with the proposed environmental pathways to chlorine oxides.[54-57] However, the relevance of oxidized chlorine reagents in prebiotic chemistry can certainly be questioned, and further investigation of the potential to accumulate and transport chlorates[55,55,57] and chlorine dioxide[56,58] would be needed to verify facile prebiotic access to **4-2P**, which we only found to be efficient by chlorite oxidation. However, it is also of note that although **4-2P** is a biological intermediate of glycolysis it is not an intermediate of our prebiotic network, rather it is a terminal node (Scheme 1; blue arrows); without the aldehyde activation exploited to yield **9**, it is difficult to envisage elimination to deliver **1** (Supplementary Fig. 1).

It is striking that the prebiotically plausible nucleotide synthesis reported by Powner *et al*,[18] is achieved, like prebiotic entry to glycolysis, through a regiochemical phosphorylation-isomer of the canonical form. Ribonucleotide synthesis,[18] occurs via 2',3'-cyclic phosphates rather than terminal 5'-phosphates, and triose glycolysis is accessed via **3-2P** rather than terminal 3'-phosphate **3-3P**. The parity of these model reaction conditions and the ostensive regiochemical switch from α-phosphorylation both suggest an integrated and unifying system to concurrently establish nucleotide synthesis and triose metabolism may have been fundamentally important in constructing the first steps towards contemporary metabolism.

Methods

Phosphorylation:

Aldehyde (25–500mM) and sodium 3-(trimethylsilyl)-1-propanesulfonate (DSS, 2.5mM) were dissolved in phosphate buffer (500mM, H_2O/D_2O 9:1, pH 4–7). Diamidophosphate (**8**; 1–4 eq.) was added and the solution was incubated at ambient temperature. ^{1}H and ^{31}P NMR spectra were

periodically acquired and phosphorylation was quantified with respect to the internal DSS standard. Aldehyde phosphates were isolated on preparative scale by ion-exchange chromatography (Dowex®-1×8, HCO_3^--form, eluent: 0 → 0.5M $Et_3NH{\cdot}HCO_3$) and barium ($Ba(OAc)_2$, 1 eq.) or calcium ($Ca(OAc)_2$, 1 eq.) salt precipitation from aqueous ethanol ($EtOH/H_2O$ 4:1) or aqueous acetone (Me_2CO/H_2O 1.2:1). Sodium salts were acquired by ion-exchange chromatography (Dowex®-50W×8, Na^+-form) followed by lyophilisation.

Glycolaldehyde 2-phosphate (**2-P**): Yield: 90% (4 eq. **8**, pH 4, 25mM, 4 h, r.t). M.p. 135–145 °C (dec). ^{1}H NMR (600 MHz, D_2O) δ_H 5.11 (1H, t, J = 4.5 Hz, (C1)-H), 3.75 (2H, dd, J = 7.4, 4.5 Hz, (C2)-H_2). ^{13}C NMR (151 MHz, D_2O) δ_C 89.9 (d, J = 7.2 Hz, C1), 67.4 (d, J = 4.9 Hz, C2). ^{31}P NMR (162 MHz, D_2O) δ_P 4.47 (t, J = 7.4 Hz). *m*/*z* (ESI-): 139 (100%, $[M-H]^+$).

Glyceraldehyde 2-phosphate (**3-2P**): Yield: 96% (4 eq. **8**, pH 4, 25mM, 4 h, r.t). M.p. 110–120 °C (dec). ^{1}H NMR (600 MHz, D_2O) δ_H 5.05 (1H, d, J = 3.8 Hz, (C1)-H), 4.09 (2H, dddd, J = 8.8, 5.7, 4.5, 3.8 Hz, (C2)-H), 3.78 (1H, ABX, J = 12.1, 4.5 Hz, (C3)-H_a), 3.75 (1H, ABX, J = 12.1, 5.7 Hz, (C3)-H_b). ^{13}C NMR (151 MHz, D_2O) δ_C 90.1 (d, J = 3.6 Hz, C1), 77.5 (d, J = 5.5 Hz, C2), 62.3 (d J = 4.4 Hz, C3). ^{31}P NMR (161 MHz, D_2O) δ_P 3.6 (d, J = 8.8 Hz). *m*/*z* (ESI+): 215 (100%, $[M-H^+]$). HRMS ($[C_3H_5O_6PNa_2+H]^+$) calcd 214.9692, found 214.9690.

Phosphoenol pyruvaldehyde (9):

A: Glyceraldehyde 2-phosphate (**3-2P**; 70mM) and pentaerythritol (10mM) were dissolved in phosphate buffer (500mM, H_2O/D_2O 9:1, pH 7) and incubated at 60 °C. NMR spectra were periodically acquired and dehydration was quantified with respect to the internal pentaerythritol standard. A maximum yield of **9** (74%) with residual **3** (12%) was observed at 23 hours.

B: Glycolaldehyde 2-phosphate (**2-P**; 80mM), formaldehyde (800mM) and DSS (15mM) were dissolved in phosphate buffer (500mM, H_2O/D_2O 9:1, pH 7) and incubated at 60 °C. NMR

spectra were periodically acquired and the yield of **9** was quantified with respect to the internal DSS standard. A maximum yield of **9** (40%) was observed at 30 hours.

Compound **9** was isolated on preparative scale by barium ($Ba(OAc)_2$, 1 eq.) salt precipitation from aqueous ethanaol ($EtOH/H_2O$ 4:1). Sodium salts were acquired by ion-exchange chromatography (Dowex®-50W×8, Na^+-form) followed by lyophilisation. An analytical sample was prepared by reversed-phase HPLC (isocratic gradient of 0.1% $NEt_3H{\cdot}HCO_3$ in water, retention time: 2.68 min). M.p. 100–115 °C (decomposed). IR (cm^{-1}, powder) 1686, 1618, 1562. ^{1}H NMR (600 MHz, D_2O) δ_H 9.25 (1H, d, J = 3.0 Hz, (C1)-H), 6.17 (1H, dd, J = 2.8, 1.8 Hz, (C3)-H_a), 5.84 (1H, dd, J = 2.8, 2.0 Hz, (C3)-H_b), 5.29 (0.04H, s, (C1)-$H^{hydrate}$), 4.87 (0.04H, $_{ap}$t, J = 2.1 Hz, (C3)-$H_2^{hydrate}$), 4.85 (1H, $_{ap}$t, J = 2.1 Hz, (C3)-$H_2^{hydrate}$), 3.18 (7H, q, J = 7.3 Hz, NC**H**$_2$CH$_3$), 1.26 (10.5H, t, J = 7.4 Hz, NCH$_2$C**H**$_3$). ^{13}C NMR (151 MHz, D_2O) δ_C 191.8 (d, J = 6.1 Hz, C1), 152.9 (d, J = 7.2 Hz, C2), 152.7 (C2^{hydrate}), 119.5 (d, J = 3.9 Hz, C3), 93.6 (C3^{hydrate}), 87.3 (C1^{hydrate}), 47.3 (N**C**H$_2$CH$_3$), 8.9 (NCH$_2$**C**H$_3$). ^{31}P NMR (161 MHz, D_2O) δ_P -4.1 ($_{ap}$s, P^{hydrate}), -4.2 ($_{ap}$s, P). *m*/*z* (ESI+): 197 (100%, $[M+H]^+$). HRMS ($[C_3H_3O_5PNa_2+H]^+$) calcd 196.9586, found 196.9583.

Aldehyde oxidation:

A: Aldehyde (30–100mM), sodium cyanide (5 eq. or none), and an internal standard (DSS, pentaerythritol, or acetate (**20**)) were dissolved in H_2O/D_2O (9:1) or D_2O and adjusted to the specified pH/pD with 1M HCl/NaOH. Cyanohydrin formation was monitored by ^{1}H NMR spectroscopy and after equilibration (0.1–1 h) the oxidant ($K_3Fe(CN)_6$, or MnO_2) was added. The solution was incubated at ambient temperature and the specified pH for 1–2 hours. The solution was filtered and NMR spectra were acquired. The carboxylic acid product was confirmed by

sample spiking and the yield (Table 1 & Supplementary Table 1) was quantified with respect to the internal standard.

B: Phosphoenol pyruvaldehyde (**9**; 25mM) and ferrous chloride (0–2 eq.) were dissolved in phosphate buffer (0.75M, H_2O, pH 10) and stirred rapidly at 0 ºC. Hydrogen peroxide (30% w/w, 1–4 eq.) was added and the reaction was stirred at 0–15 ºC for 30 min. The reaction was warmed to ambient temperature over 30 min, and the solids removed by centrifugation. The supernatant was either combined with D_2O (10% v/v) or lyophilized and re-dissolved in D_2O (1 mL). NMR spectra were acquired, and the formation of **1** was confirmed by sample spiking. The yield (Table 1 & Supplementary Table 1) was quantified with respect to an internal standard (**20**) and titration of an external standard (DSS).

C: Aldehyde (70–350mM), an internal standard (DSS or **20**) and the specified additive (none, NH_4Cl, H_2O_2, DMS, DMSO, sulfamic acid or L-methinone) were dissolved in phosphate buffer (60mM, D_2O, pH 4–7). Sodium chlorite (5M, 1.4 eq.) was added in five portions over one hour at 0 ºC, then the solution was warmed to ambient temperature and NMR spectra were acquired. The carboxylic acid product was confirmed by sample spiking and the yield (Table 1 & Supplementary Table 1) was quantified with respect to the internal standard.

Phosphoenolpyruvaldehyde cyanohydrin (**10**): ^{1}H NMR (400 MHz, D_2O, pD 9.5) δ_H 5.10 (1H, s, CH), 4.95 (1H, t, J = 1.8 Hz, CH_2), 4.83 (1H, t, J = 1.8 Hz, CH_2). ^{31}P NMR (161MHz, D_2O, pH 9.5) δ_P 0.2 ($_{ap}$s).

Phosphoenol pyruvate (**1**): ^{1}H NMR (400 MHz, D_2O, pD 4) δ_H 5.78 (1H, t, J = 2.2 Hz, (C3)-H_a), 5.44 (1H, t, J = 2.2 Hz, (C3)-H_b). ^{13}C NMR (151 MHz, D_2O) δ_C 168.1 (d, J = 7.2 Hz, C1), 146.2 (d, J = 7.2 Hz, C2), 108.6 (d, J = 3.9 Hz, C3). ^{31}P NMR (161 MHz, D_2O) δ_P -4.0 ($_{ap}$s).

Glyceric acid (**4**): ^{1}H NMR (400 MHz, D_2O, pD 4) δ_H 4.28 (1H, dd, *J* = 4.5, 3.8 Hz, CH), 3.81 (1H, ABX, *J* = 12.1, 3.8 Hz, CH_2), 3.78 (1H, ABX, *J* = 12.1, 4.5 Hz, CH_2). ^{13}C NMR (151 MHz, D_2O) δ_C 176.8 (C1), 72.3 (C2), 64.0 (C3).

Glyceric acid 2-phosphate (**4-2P**): ^{1}H NMR (400 MHz, D_2O, pD 4) δ_H 4.61 (1H, dt, *J* = 9.5, 3.6 Hz, CH), 3.89 (2H, d, *J* = 3.6 Hz, CH_2). ^{13}C NMR (151 MHz, D_2O) δ_C 175.0 (d, *J* = 3.9 Hz, C1), 75.9 (d, *J* = 5.0 Hz, C2), 63.7 (d, *J* = 5.0 Hz, C3). ^{31}P NMR (161 MHz, D_2O) δ_P 0.1 (d, *J* = 9.5 Hz).

Glycolic acid (**12**): ^{1}H NMR (400 MHz, D_2O, pD 4) δ_H 4.13 (2H, s, CH_2). ^{13}C NMR (151 MHz, D_2O) δ_C 177.4 (C1), 60.2 (C2).

Glycolic acid phosphate (**12-P**): ^{1}H NMR (400 MHz, D_2O, pD 4) δ_H 4.37 (2H, d, *J* = 8.0 Hz, CH_2). ^{13}C NMR (151 MHz, D_2O) δ_C 175.1 (C1), 63.2 (d, *J* = 5.0 Hz, C2). ^{31}P NMR (161 MHz, D_2O) δ_P 0.0 ($_{ap}$S)

Chloroacetic acid (**18**): ^{1}H NMR (400 MHz, D_2O) δ_H 4.02 (2H, s, CH_2).

Acetic acid (**20**): ^{1}H NMR (400 MHz, D_2O) δ_H 1.96 (3H, s, CH_3).

Pyruvate (6)

Phosphoenol pyruvate (**1**; 63mM) and pentaerythritol (16mM) were dissolved in H_2O/D_2O (9:1, pH 4–10), or phosphate buffer (0.5M, H_2O/D_2O, 9:1, pH 7) and incubated at 60 °C for 50 hours. ^{1}H NMR spectra were acquired periodically and the yield was quantified with respect to the internal pentaerythritol standard. Yield 95–97% (pH 4 or phosphate buffer, 50 h, 60 ºC). ^{1}H NMR (600 MHz, H_2O/D_2O 9:1, pH 4) δ_H 2.27 (3H, s, CH_3^{keto}), 1.44 (0.7H, s, $CH_3^{hydrate}$). ^{13}C NMR (151 MHz, H_2O/D_2O 9:1, pH 4) δ_C 205.2 ($C1^{keto}$), 177.2 ($C1^{hydrate}$), 170.5 ($C2^{keto}$), 93.9 ($C2^{hydrate}$), 27.1 ($C3^{keto}$), 25.9 ($C3^{hydrate}$).

Cyanohydrin/aminonitrile hydrolysis

Aldehyde (200mM), sodium cyanide (0.95–5 eq.), ammonium chloride (0–5 eq.) and DSS (20 – 25mM) were dissolved in H_2O/D_2O (9:1; adjusted to pH/pD 2, 7 or 9.5 with 4M HCl or 4M NaOH) or in phosphate buffer (750mM, H_2O/D_2O 9:1, pH 7). Cyanohydrin and aminonitrile formation were monitored by NMR spectroscopy. Upon equilibration (5–100 h), the solution was incubated at 25, 60 or 75 ºC (3–6 d) and NMR spectra were periodically acquired to monitor nitrile/amide hydrolysis. The solution was adjusted to pH/pD 12 with 4M NaOH/NaOD and incubation was continued (5–30 h). NMR spectra were periodically acquired to monitor the amide hydrolysis.

Glycolaldehyde phosphate cyanohydrin (**14**): Yield 94–98% (5 h, pH 2–9.5, r.t.). ^{1}H NMR (400 MHz, H_2O/D_2O 9:1, pH 7) δ_H 4.75 (obs., CH), 3.95 (2H, m, CH_2). ^{13}C NMR (151MHz, H_2O/D_2O 9:1, pH 7) δ_C 120.1 (C1), 65.7 (d, J = 4.4 Hz, C3), 62.3 (d, J = 6.6 Hz, C2). ^{31}P NMR (161MHz, H_2O/D_2O 9:1, pH 7) δ_P 3.8 ($_{ap}$s).

Glyceramide 3-phosphate (**15**): Yield 27% (phosphate buffer, 3 d, 75 ºC). ^{1}H NMR (600 MHz, H_2O/D_2O 9:1, pH 7) δ_H 4.25 (1H, dd, J = 5.2, 3.2 Hz, CH), 4.00 (1H, ABXY, J = 11.6, 7.6, 3.2 Hz, CH_2), 3.92 (1H, ABXY, J = 11.6, 7.6, 5.2 Hz, CH_2). ^{13}C NMR (151 MHz, H_2O/D_2O 9:1, pH 7) δ_C 179.4 (C1), 73.5 (d, J = 7.2 Hz, C2), 67.5 (d, J = 4.4 Hz, C3). ^{31}P NMR (161 MHz, H_2O/D_2O 9:1, pH 7) δ_P 4.4 (t, J = 7.6 Hz).

Glyceric acid 3-phosphate (**4-3P**): Yield 31% (phosphate buffer, 3 d, 75 ºC, then pH 12, 5h, 75 ºC). ^{1}H NMR (600 MHz, H_2O/D_2O 9:1, pH 7) δ_H 4.11 (1H, dd, J = 6.1, 2.8 Hz, CH), 3.93 (1H, ABXY, J = 11.2, 5.8, 2.8 Hz, CH_2), 3.80 (1H, ABXY, J = 11.2, 6.1, 5.8 Hz, CH_2). ^{13}C NMR (151 MHz, H_2O/D_2O 9:1, pH 7) δ_C 179.6 (C1), 73.5 (C2), 67.5 (d, J = 4.4 Hz, C3). ^{31}P NMR (161 MHz, H_2O/D_2O 9:1, pH 7) δ_P 4.0 (t, J = 5.8 Hz).

Glycolaldehyde phosphate aminonitrile (**16**): Yield 90% (pH 9.5, 100 h, r.t.). ^{1}H NMR (600 MHz, H_2O/D_2O 9:1, pH 9.5) δ_H 4.09 (1H, t, J = 5.3 Hz, CH), 3.91 (1H, ABXY, J = 10.3, 5.9, 5.3 Hz, CH_2), 3.85 (1H, ABXY, J = 10.3, 5.9, 5.3 Hz, CH_2). ^{13}C NMR (151 MHz, H_2O/D_2O 9:1, pH 9.5) δ_C 122.0 (C1), 65.4 (d, J = 4.0 Hz, C3), 44.5 (d, J = 8.4 Hz, C2). ^{31}P NMR (161 MHz, H_2O/D_2O 9:1, pH 9.5) δ_P 3.8 (t, J = 5.9 Hz).

Phosphoserinamide (**17**): Yield 65% (pH 9.5, 3 d, r.t.). ^{1}H NMR (400 MHz, H_2O/D_2O 9:1, pH 9.5) δ_H 3.86 (1H, ABXY, J = 11.6, 5.4, 5.2 Hz, CH_2), 3.84 (1H, ABXY, J = 11.6, 5.4, 5.2 Hz, CH_2), 3.65 (1H, t, J = 5.2 Hz, CH). ^{13}C NMR (151 MHz, H_2O/D_2O 9:1, pH 9.5) δ_C 178.5 (C1), 66.5 (d, J = 4.4 Hz, C3), 55.4 (d, J = 7.7 Hz, C2). ^{31}P NMR (161 MHz, H_2O/D_2O 9:1, pH 7) δ_P 4.1 (t, J = 5.4 Hz).

Phosphoserine (**5-3P**): Yield 36% (pH 9.5, 3 d, r.t., then pH 12, 3 d, 75 ºC). ^{1}H NMR (400 MHz, H_2O/D_2O 9:1, pH 12) δ_H 3.93 (1H, ABXY, J = 10.1, 4.5, 4.5 Hz, CH_2), 3.81 (1H, ABXY, J = 10.1, 6.2, 4.5 Hz, CH_2), 3.46 (1H, dd, J = 6.2, 4.5 Hz, CH). ^{13}C NMR (151 MHz, H_2O/D_2O 9:1, pH 12) δ_C 181.3 (C1), 67.9 (d, J = 5.0 Hz, C3), 57.6 (d, J = 7.7 Hz, C2). ^{31}P NMR (161 MHz, H_2O/D_2O 9:1, pH 12) δ_P 4.4 (t, J = 4.5 Hz).

[1] Eschenmoser, A. & Loewenthal, E. Chemistry of potentially prebiological natural products. *Chem. Soc. Rev.* **21**, 1–16 (1992).

[2] Jeong, H., Tombor, B., Albert, R., Oltvai, Z. N. & Barabási, A. L. The large-scale organization of metabolic networks. *Nature* **407**, 651–654 (2000).

[3] Oparin, A. I. *The origin of life.* New York, MacMillan (1938).

[4] Huber, C. & Wächterhäuser, G. Activated acetic acid by carbon fixation on (Fe,Ni)S under primordial conditions. *Science* **276**, 245–247 (1997).

[5] Miller, S. L., Schopf, J. W. & Lazcano, A. Oparin's "origin of life": sixty years later. *J. Mol. Evol.* **44**, 351–353 (1997).

[6] Morowitz, H. J., Kostelnik, J. D., Yang, J. & Cody, G. D. The origin of intermediary metabolism. *Proc. Natl. Acad. Sci. USA* **97**, 7704–7708 (2000).

[7] Zhang, X. V. & Martin, S. T. Driving parts of Krebs cycle in reverse through mineral photochemistry. *J. Am. Chem. Soc.* **128**, 16032–16033 (2006).

[8] Eschenmoser, A. On a hypothetical generational relationship between HCN and constituents of the reductive citric acid cycle. *Chem. Biodiv.* **4**, 554–573 (2007).

[9] Orgel, L. E. The implausibility of metabolic cycles on the prebiotic Earth. *PLoS Biol.* **6** 5–13 (2008).

[10] Cooper, G., Reed, C., Nguyen, D., Carter, M. & Wang, Y. Detection and formation scenario of citric acid, pyruvic acid, and other possible metabolism precursors in carbonaceous meteorites. *Proc. Natl. Acad. Sci. USA* **108**, 14015–14020 (2011).

[11] Sagi, V. N., Punna, V., Hu, F., Meher, G. & Krishnamurthy, R. Exploratory experiments on the chemistry of the ‘‘glyoxylate scenario’’: formation of ketosugars from dihydroxyfumarate. *J. Am. Chem. Soc.* **134**, 3577–3589 (2012).

[12] Patel, B. H., Percivalle, C., Ritson, D. J., Duffy, C. D. & Sutherland, J. D. Common origins of RNA, protein and lipid precursors in a cyanosulfidic protometabolism. *Nature Chem.* **7**, 301–307 (2015).

[13] De Duve, C. *Singularites: Landmarks on the pathway of life.* Cambridge University Press, Cambridge, 2005.

[14] Powner, M. W. & Sutherland, J. D. Prebiotic chemistry: a new modus operandi. *Phil. Trans. R. Soc. B* **366**, 2870–2877 (2011).

[15] Nelson, D. L. & Cox, M. M. *Lehninger principles of biochemistry.* (4th Ed.), W. H. Freeman & Co., Chapter 13, pp. 493–497 (2004).

[16] Walsh, C. T., Benson, T. E., Kim, D. H. & Lees, W. J. The versatility of phosphoenolpyruvate and its vinyl ether products in biosynthesis. *Chem. Biol.* **3**, 83–91 (1996).

[17] Potter, S. & Fothergill-Gilmore, L. A. Molecular evolution: the origin of glycolysis. *Biochem. Educ*. **21**, 45–48 (1993).

[18] Powner, M. W., Gerland, B. & Sutherland J. D. Synthesis of activated pyrimidine ribonucleotides in prebiotically plausible conditions. *Nature* **459**, 239–242 (2009).

[19] Cody et al. Primordial carbonylated iron-sulfur compounds and the synthesis of pyruvate. *Science* **289**, 1337–1340 (2000).

[20] Weber, A. The sugar model: catalysis by amines and amino acid products. *Orig Life Evol Biosph.* **31**, 71–86 (2001).

[21] Keller, M. A., Turchyn, A. V. & Ralser, M. Non-enzymatic glycolysis and pentose phosphate pathway-like reactions in a plausible Archean ocean. *Mol. Syst. Biol.* **10**, 725–737 (2014).

[22] Guzman, M. I. & Martin, S. T. Prebiotic metabolism: production by mineral photoelectrochemistry of α-ketocarboxylic acids in the reductive tricarboxylic acid cycle. *Astrobiology* **9**, 833–842 (2009).

[23] Kolb, V. & Orgel, L. E. Phosphorylation of glyceric acid in aqueous solution using trimetaphosphate. *Orig Life Evol Biosph.* **26**, 7–13 (1996).

[24] Pasek M. A., Kee, T. P., Bryant, D. E., Pavlov, A. A., & Lunine, J. I. Production of potentially prebiotic condensed phosphates by phosphorus redox chemistry. *Angew Chem. Int. Ed.* **47**, 7918–7920 (2008).

[25] Krishnamurthy, R., Arrhenius, G. & Eschenmoser, A. Formation of glycolaldehyde phosphate from glycolaldehyde in aqueous solution. *Origins Life Evol. Bio.* **29**, 333–354 (1999).

[26] Rabinowitz, J., Lores, J., Krebsbach, R. & Rogers, G. Peptide formation in the presence of linear or cyclic polyphosphates. *Nature* **224**, 795–796 (1969).

[28] Saffhill, R. Selective phosphorylation of the cis-2',3'-diol of unprotected ribonucleosides with trimetaphosphate in aqueous solution. *J. Org. Chem.* **36**, 2881–2883 (1970).

[29] Mullen L. B. & Sutherland J. D. Formation of potentially prebiotic amphiphiles by reaction of β-hydroxy-n-alkylamines with cyclotriphosphate. *Angew Chem. Int. Ed.* **46**, 4166–4168 (2007).

[29] Orgel, L. E. Prebiotic chemistry and the origin of the RNA world. *Crit. Rev. Biochem. Mol. Bio.* **39**, 99–123 (2004).

[30] Keefe, A. D. & Miller, S. L. Are polyphosphates or phosphate esters prebiotic reagents? *J. Mol. Evol.* **41**, 693–702 (1995).

[31] Sutherland, J. D., Mullen, L. B. & Buchet F. F. Potentially prebiotic Passerini-type reactions of phosphates. *Synlett* **14**, 2161–2163 (2008).

[32] Krishnamurthy, R., Guntha, S. & Eschenmoser, A. Regioselective α-phosphorylation of aldoses in aqueous solution. *Angew. Chem. Int. Ed.* ***39***, 2281–2285 (2000).

[33] Muller *et al.* Chemie von α-aminonitrilen. Aldomerisierung von glycolaldehyd-phosphat zu racemischen hexose-2,4,6-triphosphaten und (in gegenwart von formaldehyd) racemischen pentose-2,4-diphosphaten: rac-allose-2,4,6-triphosphat und rac-ribose-2,4-diphosphat sind die reaktionshauptprodukte. *Helv. Chim. Acta* **73**, 1410–1468 (1990).

[34] Eschenmoser A. Chemical etiology of nucleic acid structure. *Science* **284**, 2118–2124 (1999).

[35] Corey, E. J., Gilman, N. W. & Ganem, B. E. New methods for the oxidation of aldehydes to carboxylic acids and esters. *J. Am. Chem. Soc.* **90**, 5616–5617 (1968).

[36] Goldman, N., Reed, E. J., Fried, L. E., William Kuo, I.-F. & Maiti, A. Synthesis of glycine-containing complexes in impacts of comets on early Earth. *Nature Chem.* **2**, 949–954 (2010).

[37] Öberg *et al* The comet-like composition of a protoplanetary disk as revealed by complex cyanides. *Nature* **520**, 198–201 (2015).

[38] Osterberg, R. Origins of metal ions in biology. *Nature* **249**, 382–383 (1974).

[39] Braterman, P. S., Cairns-Smith, A. G. & Sloper, R. W. Photo-oxidation of hydrated Fe^{2+}-significance for banded iron formations. *Nature* **303**, 163–164 (1983).

[40] Liu, R. & Orgel, L. E. Oxidative acylation using thioacids. *Nature* **389**, 52–54 (1997).

[41] Keefe, A. D. & Miller, S. L. Was ferrocyanide a prebiotic reagent? *Orig. Life Evol. Biosph.* **26**, 111–129 (1996).

[42] Bowler *et al.* Prebiotically plausible oligoribonucleotide ligation facilitated by chemoselective acetylation. *Nature Chem.* **5**, 383–389 (2013).

[43] Rudnick, R. L. & Fountain, D. M. Nature and composition of the continental crust: a lower crustal perspective. *Rev. Geophys.* **33**, 267–309 (1995).

[44] Post, J. E. Manganese oxide minerals: crystal structures and economic and environmental significance. *Proc. Natl. Acad. Sci. USA* **96**, 3447–3454 (1997).

[45] Tebo *et al.* Biogenic manganese oxides: properties and mechanisms of formation. *Annu. Rev. Earth Planet. Sci.* **32**, 287–328 (2004).

[46] Hazen *et al.* Mineral evolution. *Am. Mineral.* **93**, 1693–1720 (2008).

[47] Maynard, J. B. The chemistry of manganese ores through time: a signal of increasing diversity of Earth-surface environments. *Econ. Geol.* **105**, 535–552 (2010).

[48] Trail, D., Watson, E. B. & Tailby N. D. The oxidation state of Hadean magmas and implications for early Earth's atmosphere. *Nature*, **480**, 79–82 (2011).

[49] Hazen, R. Paleomineralogy of the Hadean eon: a preliminary species list. *Am. J. Sci.* **13**, 807–843 (2013).

[50] Anbar, A. D. & Holland, H. D. The photochemistry of manganese and the origin of banded iron formations. *Geochim. Cosmochim. Ac.* **56**, 2595–2603 (1992).

[51] Chatgilialoglu, C., Crich, D., Komatsu, M. & Ryu, I. Chemistry of acyl radicals. *Chem. Rev.* **99**, 1991–2069 (1999).

[52] Kasting, J. F., Holland, H. D. & Pinto, J. R. Oxidant abundances in rainwater and the evolution of atmospheric oxygen. *J. Geophys. Res.* **90**, 10497–10510 (1987).

[53] Forsythe *et al.* Ester-mediated amide bond formation driven by wet–dry cycles: a possible path to polypeptides on the prebiotic Earth. *Angew Chem. Int. Ed.* **54**, 9871–9875 (2015).

[54] Kim, Y. S., Wo, K. P., Maity, S., Atreya, S. K. & Kaiser, R. I. Radiation-induced formation of chlorine oxides and their potential role in the origin of Martian perchlorates. *J. Am. Chem. Soc.* **135**, 4910–4913 (2013).

[55] Leshin *et al* Volatile, isotope, and organic analysis of Martian fines with the Mars Curiosity rover. *Science* **341**, 6153–6162 (2013).

[56] Solomon, S., Sanders, R. W. Garcia, R. R. & Keys, J. G. Increased chlorine dioxide over Antarctica caused by volcanic aerosols from Mount Pinatubo. *Nature,* **363**, 245–248 (1993).

[57] Jackson *et al.* Widespread occurrence of (per)chlorate in the Solar System. *Earth Planet Sci. Lett.* **430**, 470‑476 (2015).

[58] Halperin, J. & Taube, H. The transfer of oxygen atoms in oxidation-reduction reactions. III. The reaction of halogenates with sulfite in aqueous solution. *J. Am. Chem. Soc.* **74**, 375–380 (1952).

[59] Bal, B. S., Childers, W. E. & Pinnick, H. W. Oxidation of α,β-unsaturated aldehydes. *Tetrahedron* **37**, 2091–2096 (1981).

[60] Pascal, R., Taillades, J. & Commeyras, A. Strecker's and related systems. IX. Acetone as catalyst for the hydration of tertiary α-aminonitriles in aqueous basic solution. *Bull. Soc. Chim. Fr.* **2**, 177–184 (1978).

[61] Nwaukwa, S. O. & Keehn, P. M. Oxidative cleavage of α-diols, α-diones, α-hydroxyketones and α-hydroxy- and α-ketone-acids with calcium hypochlorite. *Tetrahedron Lett.* **23**, 3135–3138 (1982).

[62] Keefe, A. D., Newton, G. L. & Miller S. L. A possible prebiotic synthesis of pantetheine, a precursor to coenzyme A. *Nature* **373**, 683–685 (1995).

[63] Nargoski, R. W. & Richard, J. P. Mechanistic imperatives for aldose–ketose isomerization in water: specific, general base- and metal ion-catalyzed isomerization of glyceraldehyde with proton and hydride transfer. *J. Am. Chem. Soc.* **123**, 794–802 (2001).

Acknowledgements

We gratefully acknowledge the Simons Foundation (318881), EPRSC (EP/K004980/1), Leverhulme Trust (RGP-2013-189) and, posthumously, Harry Lonsdale for supporting this work.

Correspondence should be addressed to M.W.P. (matthew.powner@ucl.ac.uk).

Author Contributions

The research was conceived by M.W.P. Experiments were conducted by A.J.C. All authors contributed to the design and analysis of experiments, and to writing the paper.

Competing Financial Interests Statement

The authors declare no competing financial interests.

Figures and Figure Legends

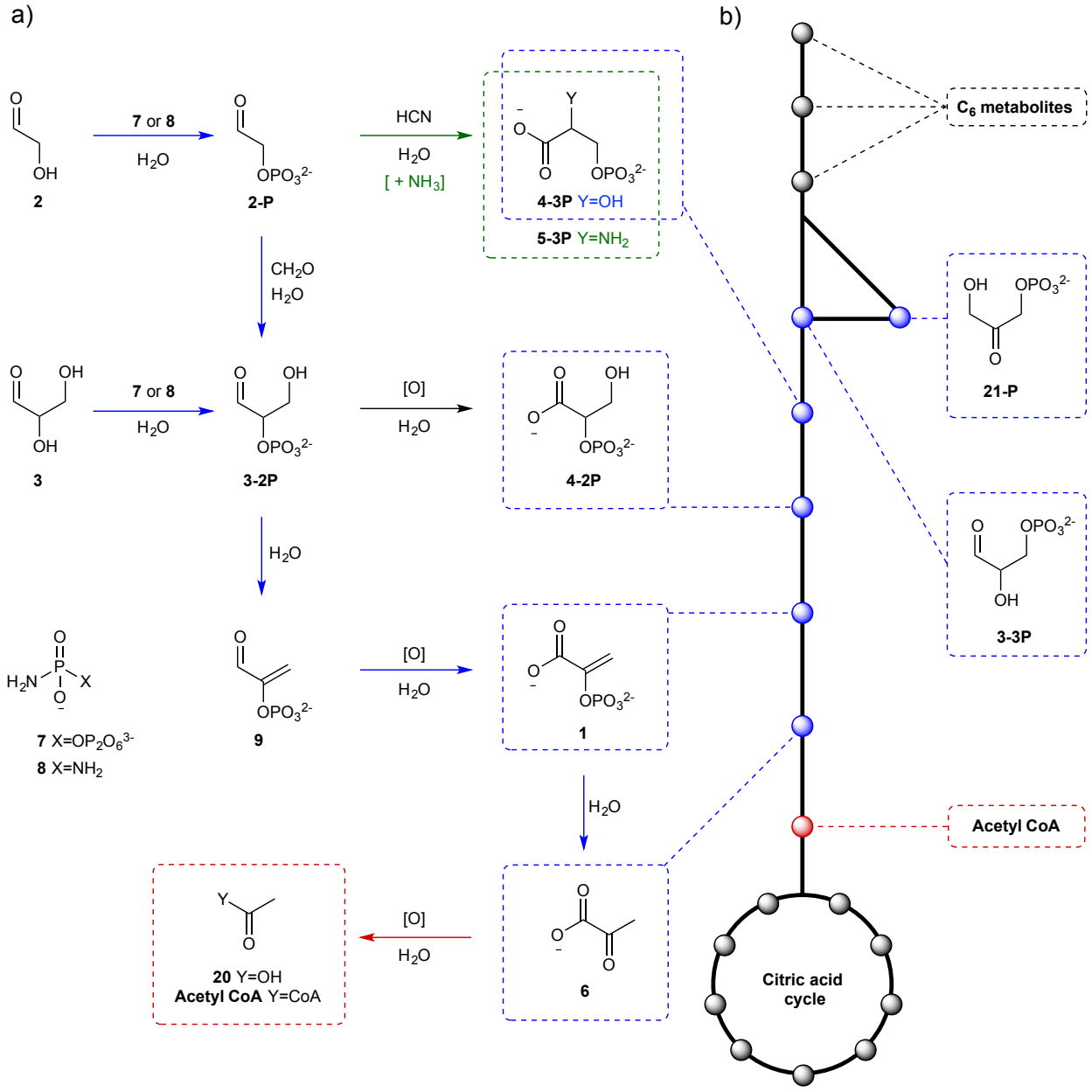

Figure 1. Reconstitution of the triose glycolysis pathway (blue nodes) in a mild prebiotically plausible aqueous reaction network controlled by α-phosphorylation. **a) Prebiotic network. Blue arrows:** Prebiotic pathway to phosphoenol pyruvate (**1**) and pyruvate (**6**) from glycolaldehyde (**2**) and glyceraldehyde (**3**). **Green arrow:** Divergent prebiotic synthesis of

glyceric acid 2-phosphate (**4-3P**; Y=O) and phosphoserine (**5-3P**; Y=NH) from glycolaldehyde-2-phosphate (**2-P**), which provides a generational link between glycolysis (blue) and serine metabolism (green). **Red arrow:** Oxidative decarboxylation of pyruvate (**6**) to yield acetate (**20**). Structures boxed (in blue) highlight the alignment between the prebiotic network and specific node on the metabolic triose glycolysis pathway. **b) Metabolic (glycolysis) network**: Enzymatically controlled pathway from C_6-metabolites to citric acid cycle via glyceraldehyde-3-phosphate (**3-3P**) and dihydroacetone phosphate (**21-P**).

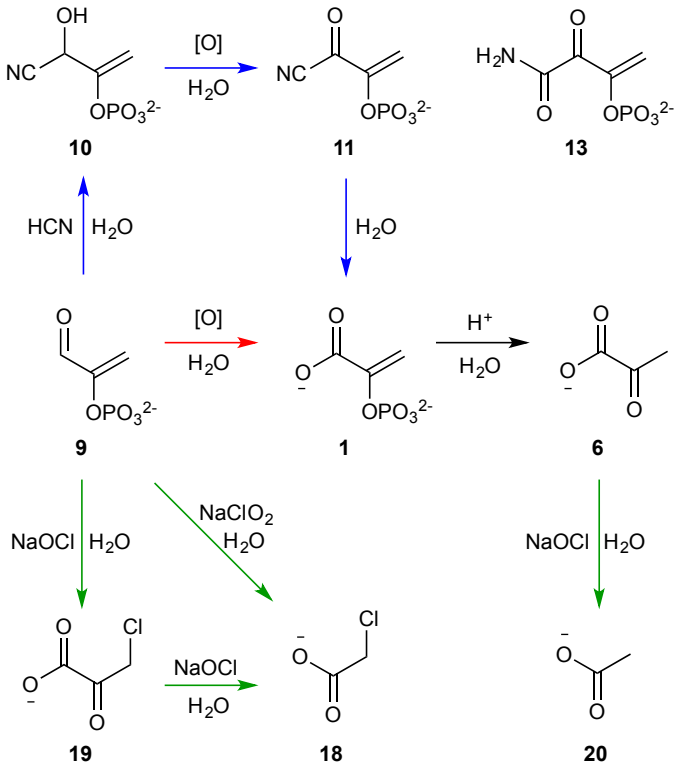

Figure 2. Oxidation of phosphoenol pyruvaldehyde (**9**) and oxidative decarboxylation of pyruvates (**6** and **19**); oxidant ([O]) and oxidation conditions are given in Table 1. **Blue arrows**: Aqueous *umpolung* oxidation of phosphoenol pyruvaldehyde (**9**) to phosphoenol pyruvate (**1**) via cyanohydrin (**10**). **Red arrow**: Direct oxidation of phosphoenol pyruvaldehyde (**9**) to

phosphoenol pyruvate (**1**). **Black arrows:** Quantitative phosphoenol pyruvate (**1**) hydrolysis. **Green arrows**: Oxidative decarboxylation of α-ketoacids (**6** and **19**) yielding acetates (**20** and **18**), respectively.

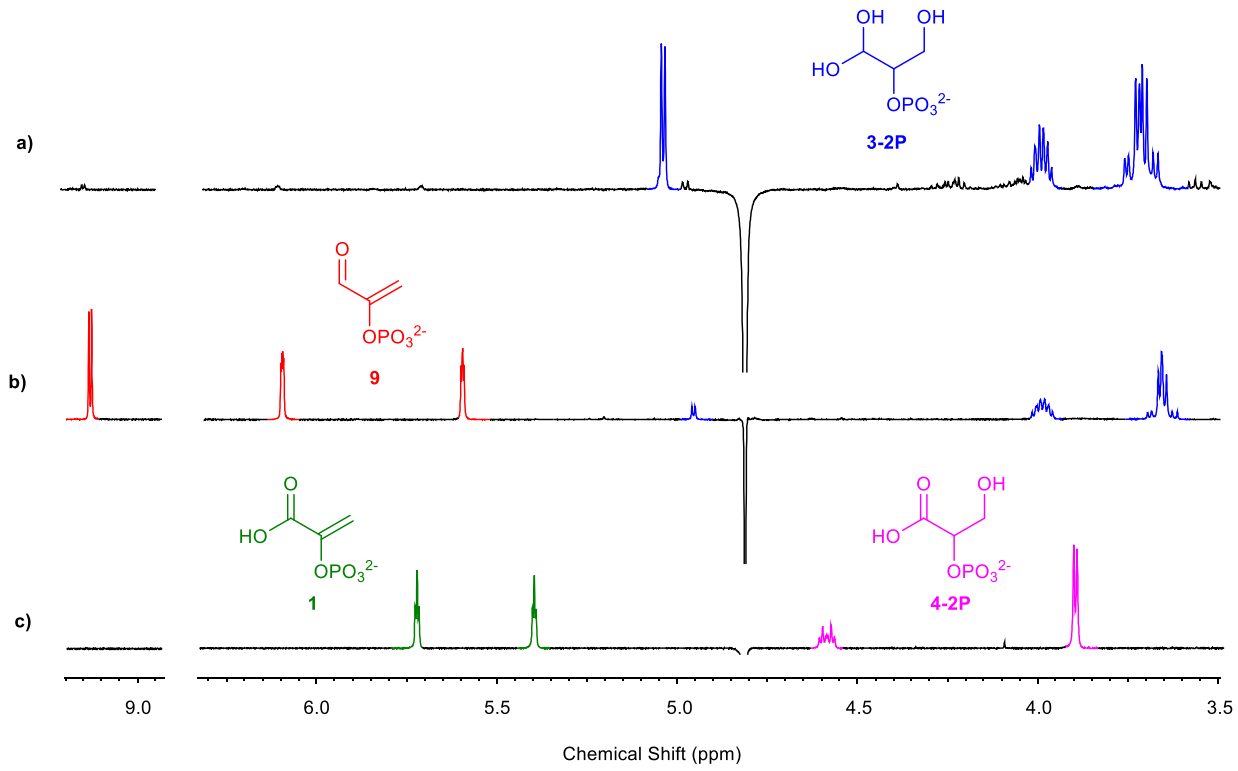

Figure 3. ^{1}H NMR spectra (600 MHz, H_2O/D_2O 9:1, 25 ºC) showing quantitative divergent synthesis of phosphoenol pyruvate (**1**)/glyceric acid 2-phosphate (**4-2P**) in 0.5M phosphate buffer. **a)** Spectrum showing the incubation of glyceraldehyde (**3**; 25mM) and diamidophosphate (**8**; 50mM) at initial pH 4 and 25 ºC for one hour in phosphate buffer, which yields glyceraldehyde-2-phosphate (**3-2P**; blue). **b)** Spectrum to show incubation of glyceraldehyde-2-phosphate (**3-2P**) in pH 7 phosphate buffer at 60 °C for five hours yielding a 1:1 mixture of glyceraldehyde-2-phosphate (**3-2P**; blue) and phosphoenol pyruvaldehyde (**9**; red). **c)** Spectrum showing the quantitative concomitant oxidation of glyceraldehyde-2-phosphate (**3-2P**) and

phosphoenol pyruvaldehyde (**1**) to glyceric acid 2-phosphate (**4-2P**) and phosphoenol pyruvate (**9**) by chlorite/DMSO (1:1.4) in pH 4 phosphate buffer at 25 ºC after one hour.

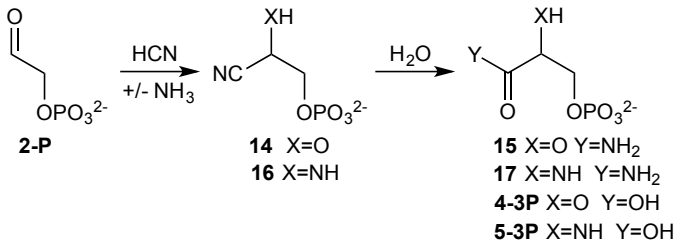

Figure 4. Divergent synthesis of glyceric acid 3-phosphate (**4-3P**) and phosphoserine (**5-3P**) from glycolaldehyde-2-phosphate (**2-P**) by quantitative cyanohydrin (**14**) or aminonitrile (**16**) formation and subsequent nitrile hydrolysis.

a) b) c)

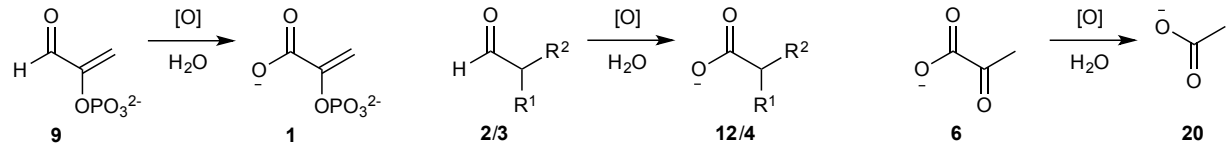

9 1 2/3 12/4 6 20

Substrate	R^1	R^2	pH	[O] (eq.)	Additive (eq.)	Product	Yield (%)
9	OPO_3^{2-}	$=CH_2$	13	$K_3Fe(CN)_6$ (10)	HCN (5)	**1** (**13**)	50 (13)
9	OPO_3^{2-}	$=CH_2$	9	MnO_2 (20)	HCN (5)	**1**	93
9	OPO_3^{2-}	$=CH_2$	10	$FeCl_2$ (1)	H_2O_2 (4)	**1 (12)**	30 (16)
9	OPO_3^{2-}	$=CH_2$	4	$NaClO_2$ (1.4)	DMSO (2)	**1**	Quant.
9	OPO_3^{2-}	$=CH_2$	4	$NaClO_2$ (2)	-	**18**	Quant.
3-2P	OPO_3^{2-}	CH_2OH	4	$NaClO_2$ (1.4)	DMSO (2)	**4-2P**	Quant.
3-3P	OH	OPO_3^{2-}	4	$NaClO_2$ (1.4)	DMSO (2)	**4-3P**	94
3	OH	CH_2OH	4	$NaClO_2$ (1.4)	DMSO (2)	**4**	93
2-P	H	OPO_3^{2-}	4	$NaClO_2$ (1.4)	DMSO (2)	**12-P**	Quant.
2	H	OH	4	$NaClO_2$ (1.4)	DMSO (2)	**12**	Quant.
6	-	-	4	NaOCl (2)	-	**20**	Quant.

Table 1. Aldehyde oxidation conditions and product yields after two hours incubation of the aldehyde and specified oxidant ([O]) in water or phosphate buffer. **a)** Oxidation of phosphoenol pyruvaldehyde (**9**) to phosphoenol pyruvate (**1**). **b)** Oxidation of glycolaldehyde (**2**) and glyceraldehyde (**3**) derivatives to glycolic acid (**12**) and glyceric acid (**4**) derivatives, respectively. **c)** Oxidative decarboxylation of pyruvate (**6**) to acetate (**20**). An expanded table of conditions and yields is provided in Supplementary Table 1.

TOC summary: Chemical reconstitution of the triose glycolysis pathway is controlled by α-phosphorylation and provides a generational link between prebiotic ribonucleotide synthesis, triose glycolysis and serine metabolism, which suggests that unification of nucleotide synthesis and triose metabolism may have been a fundamentally important step towards the origins of life.